

## Original Research

# Magnetic Resonance Image-Guided Trans-Septal Puncture in a Swine Heart

Aravind Arepally, MD,<sup>1\*</sup> Parag V. Karmarkar, MS,<sup>1</sup> Clifford Weiss, MD,<sup>1</sup>  
E. Rene Rodriguez, MD,<sup>2</sup> Robert J. Lederman, MD,<sup>3</sup> and Ergin Atalar, PhD<sup>1</sup>

**Purpose:** To test the feasibility of performing magnetic resonance (MR)-guided trans-septal punctures in the swine heart.

**Materials and Methods:** All procedures were performed in a 1.5-T MR scanner. A novel, active MR intravascular needle system was utilized for needle tracking and septal punctures. Trans-septal punctures were performed in five swine using electrocardiogram (ECG)-gated high resolution and non-ECG-gated, real-time MR imaging techniques. The intravascular needle was advanced over a guidewire from the femoral vein. Once the needle was in proper position, trans-septal punctures were made.

**Results:** Active tracking of the needle traversing the septum was possible. The location of the catheter tip was confirmed using real time gradient recalled echo (GRE). After a confirmatory ventriculogram with gadolinium-DTPA, a 0.014-inch guidewire was advanced into the left atrium and left ventricle. All punctures were made with no change in cardiac rhythm or rate; postmortem analysis was performed on all animals and demonstrated that 18/19 (95%) punctures were directly through the fossa ovalis.

**Conclusion:** Using only MR guidance and a novel active intravascular needle system, we were able to repeatedly puncture the fossa ovalis in a swine heart from a trans-femoral approach, with direct visualization of all components, including the needle, the atria, the fossa ovalis, and the surrounding vasculature.

**Key Words:** interventional; magnetic resonance imaging; trans-septal catheterization; cardiac; MR guided  
**J. Magn. Reson. Imaging 2005;21:463–467.**  
© 2005 Wiley-Liss, Inc.

THERE HAS BEEN a growing interest in the use of trans-septal catheterization of the left atrium because

of the development of balloon mitral valvuloplasty and radiofrequency catheter ablation of the pulmonary veins. Since the introduction of trans-septal punctures, the procedure has always relied upon conventional fluoroscopic techniques to guide the needle puncture. Although the technical success of this procedure under conventional fluoroscopy is high, fluoroscopy provides only indirect anatomic information and is forced to rely on secondary anatomic localizers to define a safe needle trajectory. Examples of this include biplane fluoroscopy in conjunction with a pigtail catheter in the aorta and the use of His bundle/coronary sinus catheters (1), and, more recently, the use of intracardiac echocardiography (2).

Due to the increased speed of magnetic resonance (MR) acquisition and the development of device/catheter tracking technology, MRI has been explored as an alternative for various vascular procedures. The ability to perform MRI-guided trans-septal punctures would provide a novel approach to these procedures by uniting real-time, high resolution anatomic and functional imaging during diagnostic and therapeutic interventions, making feasible such procedures as MRI-guided pulmonary vein ablations, mitral valve repair, and other intracardiac applications. The purpose of our study was to demonstrate that MRI-guided trans-septal puncture and catheterization of the left atrium is safe and feasible from a percutaneous femoral vein approach.

## MATERIALS AND METHODS

### Animal Model

The Institutional Animal Care and Use Committee approved all animal studies. Experiments were performed on five healthy swine (40–45 kg). Sedation was achieved with xylazine and ketamine. After endotracheal intubation, inhaled isoflurane (2%) was provided during mechanical ventilation with oxygen (98%). Using ultrasound guidance, percutaneous access into the right femoral vein was achieved with an 11-French sheath. All animals were then transferred to the MR suite for the remaining portion of the procedure.

### Trans-Septal Needle

A schematic of the active MR needle, which is manufactured in our laboratory, is shown in Fig. 1a and b.

<sup>1</sup>The Russell H. Morgan Department of Radiology and Radiological Science, The Johns Hopkins Medical Institutions, Baltimore, Maryland.

<sup>2</sup>Department of Pathology, Johns Hopkins University School of Medicine, Johns Hopkins Medical Institutes, Baltimore, Maryland.

<sup>3</sup>Cardiovascular Branch, Division of Intramural Research, National Heart Lung and Blood Institute, National Institutes of Health (NIH), Bethesda, Maryland.

Contract grant sponsor: NIH; Contract grant number: R01 57483; Contract grant sponsor: American Roentgen Ray Scholarship.

\*Address reprint requests to: A.A., Cardiovascular/Interventional Radiology, The Johns Hopkins Hospital, Blalock 545, 600 N. Wolfe Street, Baltimore, MD 21287. E-mail: aarepal@jhmi.edu

Received September 7, 2004; Accepted November 22, 2004.

DOI 10.1002/jmri.20262

Published online in Wiley InterScience (www.interscience.wiley.com).

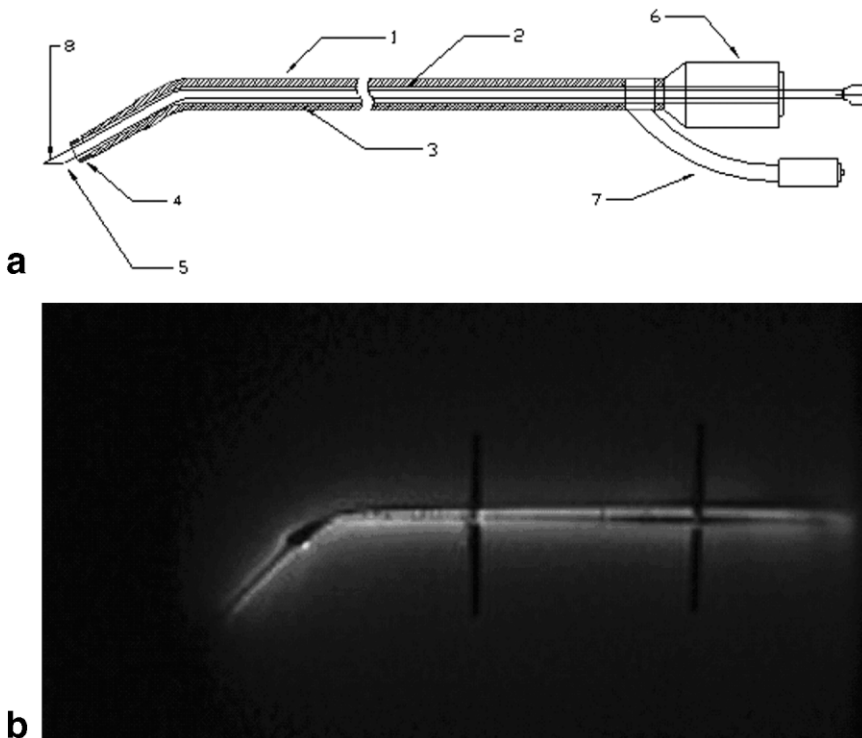


**Figure 1.** **a:** 1) outer nitinol tube, 2) inner nitinol tube with a polyimide liner, 3) nylon dielectric, 4) copper wire coil, 5) three-face bevel, 6) connector for syringe, 7) coaxial cable connector to interface circuit, and 8) removable nitinol puncture needle. **b:** An image acquired of the needle in a saline phantom using a fast gradient echo pulse sequence.

This needle is made of concentrically configured nitinol hypotubings arranged to form a loopless antenna (3). The end of the needle is preshaped at the distal tip to provide a 55° bend, which results in a needle trajectory that is perpendicular to the caval wall. The inner lumen of the inner tube is insulated with a liner that electrically insulates the system and acts as a guidewire lumen (0.038-inch wire-compatible). The entire assembly is insulated in nylon in order to isolate the needle components from direct electrical contact with biologic fluids. The loopless antenna is matched to 50 ohms at 63.86 MHz. The coaxial introduction of a second nitinol guidewire (0.014-inch) tip, which is sharpened, is used to puncture the fossa ovalis.

### MRI-Guided Trans-Septal Puncture

All trans-septal punctures were performed solely under MRI guidance in a 1.5-T MR scanner (CV/i; GE Healthcare Waukesha, WI). Images were acquired using a combination of external phased array coils and the intravascular needle. The needle was introduced from the common femoral vein and advanced over a 0.035-inch nitinol guidewire (EV3, Plymouth, MA). Using a real-time GRE sequence (Fig. 2a and b) in combination with an interactive scan plane acquisition (i-Drive, GE), the needle was advanced into the right atrium. After the needle was oriented at the septum, an electrocardiogram (ECG)-gated fast imaging employing steady-state acquisition (FIESTA) sequence was acquired (Fig. 2c and d) using a four-chamber view and an oblique coronal view that visualized the inferior vena cava (IVC) and foramen ovale. Next, under a real-time GRE sequence, the needle system was guided from the right atrium through the septum and into the left atrium with free breathing and without ECG gating (Fig. 2e and f). The

location of the distal tip of the needle was then confirmed by an ECG-gated FIESTA sequence (Fig. 2g and h). Following the puncture, a 0.014-inch guidewire was advanced into the left atrium and left ventricle (Fig. 3a and b). A confirmatory ventriculogram, using 5 cc of gadolinium-DTPA, was also performed using a fast spoiled gradient echo sequence (6 msec TR, 1.3 msec TE, 90° flip angle, no slice selection, 45 cm field of view [FOV], 256 × 256 image matrix, number of excitations [NEX] = 1, and 1.5 frames/second; Fig. 3c). After the procedure, the explanted hearts from all animals were fixed with unpressurized formalin. Postmortem examination was performed to evaluate the septal punctures (Fig. 3d).

### RESULTS

Trans-septal puncture into the left atrium was successfully performed in all five swine. During the procedure, the interventionist (A.A. or C.W.) advanced the needle while monitoring the needle position using an imaging console adjacent to the MRI scanner. The MRI scanner was operated to control imaging parameters and slice orientation, based on the feedback of the interventionist. Punctures were made with no change in cardiac rhythm or rate and with no sequelae. A total of 19 punctures (one pass only per puncture) were made in five animals and each was confirmed with a ventriculogram using gadolinium-DTPA.

Three standard views were used with the real-time sequence with each puncture. An oblique coronal view of the IVC and right atrium was used to track the needle's entry into the atrium and provide directionality and orientation of the needle. A true short axis and four-chamber view of the heart was used to identify the

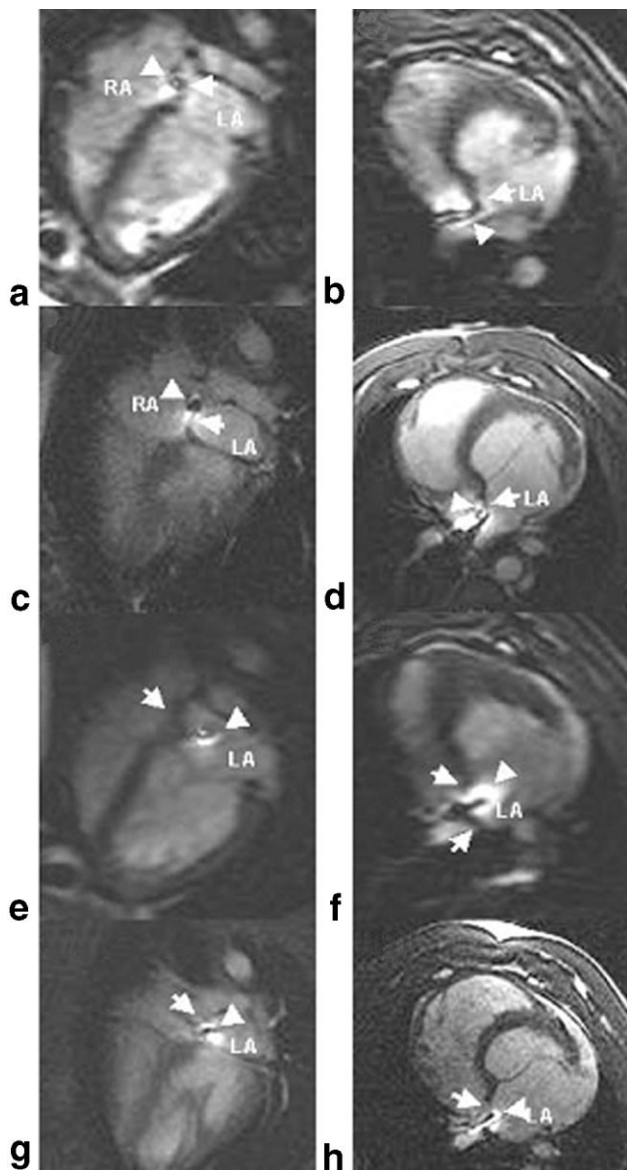


**Figure 2.** Monitoring the process of atrial septal puncture. **a-d:** Visualization of the tip of the needle within the right atrium adjacent to and pressing on the fossa ovalis. **e-h:** Active needle tip within the left atrium after having passed through the fossa ovalis. **a, c, e, and g:** Four-chamber views. **b, d, f, and h:** Axial views. Images **c, d, g, and h** were acquired using a FI-ESTA sequence (TR = 3.5 msec, TE = 1.0 msec, flip angle = 60°, bandwidth = 125 kHz, slice thickness = 7 mm, FOV = 35 cm, matrix size = 256 × 256, and NEX = 1) to verify the position accurately. Images **a, b, e, and f** were acquired with a real-time sequence (TR = 3.4 msec, TE = 1.2 msec, flip angle = 45°, bandwidth = 125 kHz, slice thickness = 10 mm, FOV = 30 cm, image matrix size = 128 × 128, and NEX = 1) and were used to guide the procedure.

relationship of the needle to the fossa ovalis, the aorta, and all four cardiac chambers. During the procedure, the interventionist was able to rapidly change to any of these prescribed planes. All punctures were made with the short axis view and an immediate return of bright blood was noted from the needle hub in all punctures. The typical duration of each puncture was approxi-

mately 10 minutes. This time period was begun during the insertion of the needle into the femoral vein and ended once the confirmatory ventriculogram was performed.

Pathology of all explanted hearts demonstrated that 18/19 (95%) punctures went directly through the center of the fossa ovalis. One puncture entered the left atrium just superior to the limbus of the fossa ovalis. There was no direct visual evidence of thermal injuries. No injury to the right or left atrium was noted. (Fig. 3d).

## DISCUSSION

Due to the invasiveness of a trans-septal procedure and the potential for vascular or cardiac injury, we developed an active MR intravascular needle that can be completely visualized in an MR environment and can be used to perform MRI-guided punctures of the fossa ovalis. In addition to monitoring the needle, we were able visualize all cardiac chambers, pertinent vascular structures, and the fossa ovalis in order to safely perform this procedure. Using this needle in combination with real-time (non-ECG-gated, free breathing) and standard cardiac MRI imaging (ECG-gated) allowed for adequate temporal and spatial resolution so that active tracking of the needle during trans-septal punctures was possible. With pathologic confirmation, we demonstrated that 18/19 (95%) punctures were directed entirely through the fossa ovalis with no sequelae with regard to cardiac rhythm or rate.

Due to advances in gradient hardware and the development of MR-visible guidewires and catheters, steady progress has been made in performing MRI-guided cardiovascular procedures (4). Successful coronary artery catheterization and stenting under MRI guidance have been described, using both a carotid (5,6) and a femoral artery approach (7). In addition, using MR fluoroscopy, directed injections of dilute gadolinium-DTPA and mesenchymal stem cells into normal and injured left ventricular myocardial tissue was shown to be technically feasible (8,9).

Newer clinical applications that require extensive fluoroscopy and complex anatomic imaging may benefit the most from MRI guidance. Rickers et al (10) demonstrated the closure of artificially created atrial septal defects in swine by delivering the Amplatzer septal occluder under MRI guidance. The passive artifact from the nitinol mesh provided adequate contrast to deploy the device across the septal defect. However, in this study, the septal punctures were performed under fluoroscopy while the device was advanced across the septal defect under MRI guidance. In addition, real-time MRI has been described to facilitate precise anatomic radiofrequency ablations of right ventricular tissue by Lardo et al (11). Their study also confirmed that the biophysical effects of these ablations could be seen with standard MRI sequences. In another study, Dickfeld et al (12) successfully performed right atrial catheter ablations using data from previously acquired MRI anatomic datasets and a stereotactic catheter guidance system. However, since this technique uses prior MRI data, this procedure may not compensate for cardiac or respiratory motion and would have limitations in a clin-

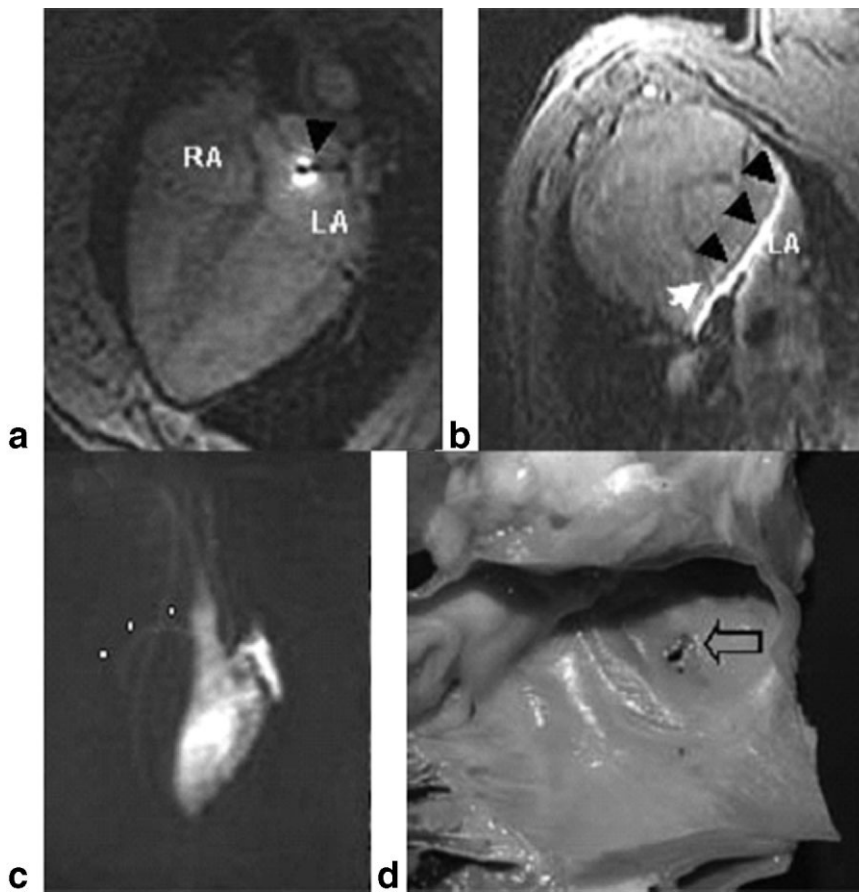


**Figure 3.** Images (four-chamber view [a], short axis view [b]) demonstrate a wire that has been passed into the left atrium through the fossa ovalis. **c:** Left ventriculogram obtained after the injection of gadolinium through the septal puncture needle, which demonstrates the left atrium, left ventricle, aorta, and coronary arteries. Note that there is no filling of the right atria or ventricle. **d:** Gross pathologic photo of the fossa ovalis viewed from the left atrium. Block arrow indicates the atrial septal punctures. Images a and b were fast gradient echo (TR = 5.6 msec, TE = 1.5 msec, flip angle = 25°, bandwidth = 125 kHz, slice thickness = 7 mm, FOV = 35 cm, matrix size = 256 × 256, and NEX = 1). RA = right atrium, LA = left atrium, small arrow = active needle tip, large arrow = fossa ovalis, black arrows = inactive wire, circles = right coronary artery.

ical situation. Finally, since performing MRI-guided trans-septal punctures was not feasible, all prior MRI-guided ablation research has been performed in the right heart only.

Due to the temporal resolution of x-ray fluoroscopy, current techniques for trans-septal puncture and catheterization can be performed safely and quickly. Limitations to conventional x-ray include ionizing radiation and the need for iodinated contrast; in addition, fluoroscopy provides very limited luminal anatomy of cardiovascular structures. MRI-guided trans-septal punctures offer a novel alternative and provide several advantages over conventional fluoroscopy. In addition to vastly improved soft tissue resolution, the capabilities of real-time, multiplanar/three-dimensional anatomy allowed for unsurpassed depiction of the fossa ovalis, cardiac chambers, and vascular anatomy, without the need for radiation or potentially nephrotoxic contrast. Furthermore, direct visualization of the needle and its relationship to the fossa ovalis provided for a safe and direct needle trajectory without the need for additional catheters or equipment. Finally, the ability to perform MRI-guided trans-septal punctures would provide a novel approach to achieve a more comprehensive cardiovascular procedure that would unite high resolution anatomic and functional imaging to deliver and monitor a myriad of therapies. Procedures such as MRI-guided pulmonary vein ablations, mitral valvular repair, and other intracardiac applications may become feasible.

Currently, there are several limitations with this technique. Since this is a first-generation device, local

heating properties on the adjacent soft tissues have not been fully evaluated. Although we did not see any direct thermal injuries on gross pathology, RF specific absorption rate (SAR) safety issues have not yet been fully analyzed. We plan to measure the safety index, the expected temperature increase caused by the needle for a given unit of (SAR) distribution, and adjust the power level accordingly (13). We plan to use safety index reduction methods such as insulation and utilization of balun circuits. In addition, in our study, we found that one puncture entered the left atrium just superior to the limbus of the fossa ovalis. This improper puncture may have been related to operator error and may have occurred due to the small size of the fossa ovalis in the swine heart. We strongly believe that with the increase in our experience with this technique, as well as improvements and modifications of current needle systems and MR imaging techniques, the success rate will further increase.

In conclusion, using MR guidance and a novel active intravascular needle system, we were able to successfully and safely puncture the fossa ovalis of a swine heart from a transfemoral approach with direct visualization of all components including the needle, the fossa ovalis, the atria, and the surrounding vasculature.

## REFERENCES

1. Gonzalez MD, Otomo K, Shah N, et al. Transseptal left heart catheterization for cardiac ablation procedures. *J Interv Card Electrophysiol* 2001;5:89–95.

2. Daoud EG, Kalbfleisch SJ, Hummel JD. Intracardiac echocardiography to guide transseptal left heart catheterization for radiofrequency catheter ablation. *J Cardiovasc Electrophysiol* 1999;10:358–363.
3. Ocali O, Atalar E. Intravascular magnetic resonance imaging using a loopless catheter antenna. *Magn Reson Med* 1997;37:112–118.
4. Lardo AC. Real-time magnetic resonance imaging: diagnostic and interventional applications. *Pediatr Cardiol* 2000;21:80–98.
5. Serfaty JM, Yang X, Aksit P, et al. Toward MRI-guided coronary catheterization: visualization of guiding catheters, guidewires, and anatomy in real time. *J Magn Reson Imaging* 2000;12:590–594.
6. Spuentrup E, Ruebben A, Schaeffter T, et al. Magnetic resonance-guided coronary artery stent placement in a swine model. *Circulation* 2002;105:874–879.
7. Omary RA, Green JD, Schirf BE, et al. Real-time magnetic resonance imaging-guided coronary catheterization in swine. *Circulation* 2003;107:2656–2659.
8. Lederman RJ, Guttman MA, Peters DC, et al. Catheter-based endomyocardial injection with real-time magnetic resonance imaging. *Circulation* 2002;105:1282–1284.
9. Dick AJ, Guttman MA, Raman VK, et al. Magnetic resonance fluoroscopy allows targeted delivery of mesenchymal stem cells to infarct borders in Swine. *Circulation* 2003;108:2899–2904.
10. Rickers C, Jerosch-Herold M, Hu X, et al. Magnetic resonance image-guided transcatheter closure of atrial septal defects. *Circulation* 2003;107:132–138.
11. Lardo AC, McVeigh ER, Jumrussirikul P, et al. Visualization and temporal/spatial characterization of cardiac radiofrequency ablation lesions using magnetic resonance imaging. *Circulation* 2000;102:698–705.
12. Dickfeld T, Calkins H, Zviman M, et al. Anatomic stereotactic catheter ablation on three-dimensional magnetic resonance images in real time. *Circulation* 2003;108:2407–2413.
13. Yeung CJ, Susil RC, Atalar E. RF safety of wires in interventional MRI: using a safety index. *Magn Reson Med* 2002;47:187–193.